

CHAPTER - IV

MAGNETIZATION OF Mg-Co FERRITES

CHAPTER - IV

MAGNETIZATION OF Mg-Co FERRITES

INTRODUCTION

Ferrites is a broad class of ceramic materials, which combines the resistivity of good insulators with high permeability. These are artificially prepared magnets hence their magnetization can be varied by altering their composition. Crystallographically, these are different from ferromagnetic materials in that their magnetic ions are distributed over at least two interpenetrating sublattices. In behaviour, these ferrimagnets are quite similar to ferromagnets.

The hysteresis study of ferrites gives information about permeability, saturation magnetization, coercive field and remanance ratio. Magnetical importance of ferrites lies in their values of coercive field and permeabilities on which broad spectrum of application depends. The coercive force of ferrites ranges from 0.1 Oe to 3 KOe; depending upon porosity, anisotropy, internal stresses and saturation magnetization [1]. Ferrites having low coercive field values are called as "soft ferrites " and those with high coercive force are called as "hard ferrites".

The factors governing magnetic and hysteresis properties of ferrites are chemical composition, preparation conditions and heat treatment. The presence of impurities and grain size also affect the magnetic properties [2], [3].

The present study includes the variation of magnetization with sintering time for Mg-Co ferrites.

4.1 MAGNETISM

The origin of magnetism lies in the motion of orbiting electrons. The motion can be divided into two parts, the orbital motion of electron about the nucleus and a spin of electron about its own axis. Both the types of motions contribute to the total angular momentum and magnetic moment is proportional to the angular momentum. The relative importance of spin and orbital motion varies considerably from one type of atom to the next, depending on the electronic configurations of each atom and its environment. In case of solid crystalline materials the local crystalline field causes rapid precession of electron orbit about the nucleus. This averages out the orbital motion of the most ions so that only contributions due to spin magnetic moment are operative. Although each electron has a magnetic moment associated with its spin motion (and possibly orbital motion), the magnetic behaviour of an atom or ions depends on combination of the moment contribution from different electrons. Depending on the combination of magnetic moment contributions of different

electrons, broadly, substances can be classified as diamagnetic or paramagnetic. In diamagnetic substance, contributions due to different electrons are exactly paired off so that magnetic moments get balanced and the substances become nonmagnetic. In paramagnetic substances, spin due to each electron cannot be paired off and hence the substances have a net unbalanced electronic spin. These substances are magnetic in nature.

The spin arrangements in atoms helps us to distinguish between paramagnetism, ferromagnetism, antiferromagnetism and ferrimagnetism.

In paramagnetic substances the spins are randomly oriented due to weak interaction between ions or disordered spin structure is observed. Parallel spin arrangements are found in ferromagnetic substances. The strong internal field which aligns the spins is called "Weiss molecular field" [4]. The order of magnitude of molecular field is 10^5 to 10^7 Oe. The ferromagnetism in metals is produced mainly by direct exchange mechanism. Compensated antiparallel spins result in antiferromagnetic behaviour whereas ferrimagnetism is due to uncompensated spins. Ferrimagnetic materials exhibit greater magnetization.

4.2 BASIC POSTULATES OF MAGNETIZATION

4.2.1 Magnetic Terms

Magnetic substances either attract or repel other substances even though the two are not in contact. This action at a distance takes place due to 'lines of force' constituting magnetic flux Φ . The induced magnetism or magnetic induction in substance is flux per unit area ie.

$B = \frac{\Phi}{A}$ If B is the induction produced due to applied field

H, then $B = \mu H$, where μ is the permeability. If a substance acquires magnetic moment, it gets magnetized under the applied field H. The intensity of magnetization is the average moment per unit volume or it is pole strength (m) per unit area of cross section ie $M = m/A$.

The field due to induced moment is $4\pi M$. Thus magnetic induction can be expressed as,

$$\text{Hence } \left. \begin{aligned} B &= H + 4\pi M \\ \frac{B}{H} &= 1 + 4\pi \frac{M}{H} \\ \mu &= 1 + 4\pi \chi \end{aligned} \right\} \quad (4.1)$$

The term,

$\chi = \frac{M}{H}$, intensity of magnetization per unit field is

called as susceptibility.

According to mean field approximation, the molecular field is proportional to magnetization M

$$B_M = \lambda M \quad (4.2)$$

The constant λ is molecular field coefficient. The Curie temperature is transition temperature which separates the paramagnetic phase at $T > T_C$, from ordered ferromagnetic phase $T < T_C$ [5].

The temperature variation of susceptibility is given by Curie Wiess law as,

$$\chi = \frac{C}{T - T_C} \quad (4.3)$$

Where

C = Curie constant

T_C = Transition or the Curie temperature.

4.2.2 Molecular Field and Exchange Forces

The hypothesis that, B_M is proportional to magnetization indicates that some cooperative phenomenon is involved in the origin of molecular field. Thus when degree of spin alignment in a particular region of the crystal is greater, the force tending to align any one spin in that direction is greater [6]. The molecular field is entirely magnetic due to spin-spin interactions which are purely magnetic in nature.

In 1925, Heisenberg showed that, molecular field is caused by quantum mechanical exchange force [7]. The exchange

of spinning electrons between the two neighbouring atoms give rise to exchange force and exchange energy. The charge distribution of a system of two spins depend on whether the spins are parallel or antiparallel, due to the fact that, Pauli's principle restricts two electrons of the same spin from being at the same place at same time. It does not exclude two electrons of opposite spins.

The exchange energy is very important part of total energy. For the atoms i and j having spin angular moment $S_i \frac{h}{2\pi}$ and $S_j \frac{h}{2\pi}$ the energy is given by,

$$\left. \begin{aligned} E_{ex} &= - 2 J_{ex} S_i \cdot S_j \\ &= - 2 J_{ex} S_i S_j \cos \phi_{ij} \end{aligned} \right\} \quad (4.4)$$

Where ϕ_{ij} is the angle between spin vectors S_i, S_j and J_{ex} is an 'Exchange integral'. Total energy W_{ex} is obtained on summation

$$W_{ex} = 2 J_S^2 \sum_{i \neq j} \cos \phi_{ij} \quad (4.5)$$

Where 'S' is the total spin momentum and J is total exchange integral. J_{ex} can be positive or negative. If J_{ex} is positive and spins are parallel, for $\cos \phi = 1$ E_{ex} is minimum and for antiparallel spins as $\cos \phi = - 1$ E_{ex} is maximum. When J_{ex} is negative, the lowest energy states result from antiparallel spins. Ferromagnetism is due to alignment of

spin moments on adjacent atoms. For ferromagnetism the value of exchange integral must be positive. J_{ex} is commonly negative. Positive J_{ex} is rarely found. Therefore only few substances are ferromagnetic. According to older Weiss theory, ferromagnetism is caused by powerful "Molecular field" which aligns the atomic moments but recently it is considered that, exchange forces aligns the spin parallel, antiparallel or unbalanced parallel to give magnetic properties.

4.3 FERROMAGNETIC DOMAINS

The fact that saturation does not occur in ferromagnetic substance when it is subjected to small field implies that, elementary magnets are not entirely free but are impeded by something. In the whole specimen spontaneous moment appears to be less than the saturation moment and only the application of external field may saturate the specimen. According to Weiss theory any magnetic specimen is constituted by small regions or small zones called "domains" in which the local magnetization is saturated. These domains are randomly oriented. Sometimes the domains are closed, giving zero resultant magnetization. Under the application of external field the domains undergo orientation. The net magnetization exhibited in the presence of some applied field is the result of orientation of magnetic domains in the direction of the applied field. According to Landau and Lifshitz [8] the

formation of domain is due to the minimization of magnetic energy. The total magnetic energy is the sum of magnetostatic, magnetostrictive, anisotropy and exchange energy. Domain walls are the interfaces between the regions in which, spontaneous magnetization has different directions. Within the walls, the magnetization must change the direction. Since the spins within the walls are orienting in noneasy directions, the crystal anisotropy energy of the wall is higher than that of adjoining domains. As the exchange energy tries to widen the wall, to reduce the angle ϕ between the spins, the anisotropy energy tries to make the wall thinner so as to reduce the number of spins pointing in noneasy direction. Due to this the wall has a finite width and certain structure. Bloch in 1932, studied theoretically the structure of domain wall, hence it is called as Bloch wall. Its thickness is of the order of few hundred interatomic distances. The spin rotation helps to classify the walls in two types ie 180° and 90° walls.

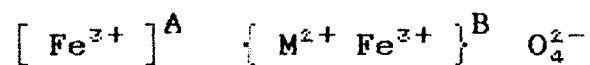
For polycrystalline materials, domain structures for each grain are similar to large crystals. The modification of domain structure is due to small dimensions of grains and the interaction between the adjoining grains [9].

4.4.1 MAGNETIZATION IN FERRITES

Ferrites exhibit magnetic behaviour because of the distribution and alignment of magnetic ions on octahedral and tetrahedral sites. The cations sitting on the same sublattice are so oriented that their magnetic moments are in same direction. For two sublattices, the moment of cations on one sublattice are aligned antiparallel to the moment of cations on the other sublattices. The resultant magnetization of the two sublattices is the effective magnetization of the crystal.

4.4.2 STRUCTURAL EXPLANATION OF FERRIMAGNETISM

In general, magnetic ferrites possess inverse spinel structure. The cation distribution is thus given by, [10]



The cations shown in square bracket are on A sites and in curly bracket are on B sites. Since the ferrite unit cell consists of eight molecules, on the A sublattice the moments of 8Fe^{3+} cations are located while on the B sublattice the moments of $8(\text{Fe}^{3+} + \text{M}^{2+})$ cations are located, per unit cell. The resultant magnetization is given by

$$\begin{aligned} M &= |M_B - M_A| \\ &= 8 (m_M + m_{\text{Fe}}) - 8m_{\text{Fe}} \\ &= 8 m_M \end{aligned}$$

Where, M_A and M_B are the moments of the sublattices. m_M and m_{Fe} are the spin magnetic moments of the individual ions. The parallel alignment of moments on each sublattice is a result of superexchange interaction between the magnetic ions on one sublattice and those on the other.

The parallel alignment of each sublattice which is characteristic of ferrimagnetism, requires sufficient concentration of the magnetic species on each sublattices. Ferrites with normal spinel structures (like $ZnFe_2O_4$ and $CdFe_2O_4$) are nonmagnetic. In these ferrites the A-B interaction does not exist, as there are no magnetic ions on the A sites, the B-B interaction lines up half in the opposite direction so that alternate planes of B sublattice are magnetized in opposite direction rendering these ferrites non magnetic. Due to superexchange [11] interaction between two cations via an intermediate oxygen ion, if the three ions are collinear, and their separation are not too large, the sublattice magnet ions are antiparallel [12]. The net magnetic moment per formula unit of an inverse ferrite structure cannot exceed 5 Bohr magnetons. The addition of normal spinel ferrites like $ZnFe_2O_4$ increases the magnetic moment of inverse ferrite, since on addition the nonmagnetic ions occupy A sites and equal number of Fe^{3+} ions are transferred to B sites.

4.5 a) NEEL' S THEORY OF FERRIMAGNETISM

Using the same approach as that used for Weiss molecular field theory of ferromagnetism, Neel formulated the theory of antiferromagnetism. Neels theory of antiferromagnetism allows to determine the Curie constant and molecular field constants that describe the antiferromagnetism. When the two magnetic sublattices in a magnetic substances are antiparallel as in the antiferromagnetic substances but their magnetization is different so that it cannot be compensated, material is called as ferrimagnetics. In a simple ferrimagnetic substance either there are two sublattices occupied by the magnetic ions with different spin magnetic moments or the same magnetic ions being located on crystallographically different sites, forming two sublattices. Both these effects may be present simultaneously in various ferrites.

Neel putforward the concept of negative interactions between the ions on A site and B sites to explain the antiparallel alignment of moments. Besides A-B interaction, A-A and B-B interactions are taken into account although they are weak negative interactions. The molecular field acting on an atom at A site and B-site is given by,

$$\text{and } \left. \begin{aligned} H_{ma} &= -\gamma_{aa} M_A - \gamma_{ab} M_B \\ H_{mb} &= -\gamma_{bb} M_B - \gamma_{ba} M_A \end{aligned} \right\} \quad (4.6)$$

Where,

γ 's are appropriate molecular field constants.

M_A = Magnetization of A lattice

M_B = Magnetization of B lattice

At equilibrium $\gamma_{ab} = \gamma_{ba}$. But in ferrimagnetics the sublattices are crystallographically inequivalent, making $\gamma_{aa} \neq \gamma_{bb}$. Unless two sublattices are identical, $\gamma_{ab} > 0$ favouring antiparallel alignment of M_A and M_B giving rise to net magnetization of ferrimagnets. In the presence of external field (H), total magnetic field acting on an atom in each lattice is given by,

$$\left. \begin{aligned} H_A &= H - \gamma_{aa}M_A - \gamma_{ab}M_B \\ H_B &= H - \gamma_{bb}M_B - \gamma_{ba}M_A \end{aligned} \right\} \quad (4.7)$$

i) Paramagnetic Region

The sublattice magnetization, for an assembly of N atoms per unit volume, each with angular momentum number J are represented by,

$$\text{and} \quad \left. \begin{aligned} M_A &= \frac{C_a}{T} H_{ma} \\ M_B &= \frac{C_b}{T} H_{mb} \end{aligned} \right\} \quad (4.8)$$

Where,

$$\left. \begin{aligned} C_a &= \sum_i N_i g^2 \mu_B^2 S_i (S_i + 1) \\ C_b &= \sum_j N_j g^2 \mu_B^2 S_j (S_j + 1) \end{aligned} \right\} \quad (4.9)$$

here N_i and N_j are number of atoms per unit volume with spin quantum numbers S_i and S_j respectively,

g = Lande's factor

μ_B = Bohr magneton

Now, the volume susceptibility can be defined as,

$$\chi = \frac{M_A + M_B}{H} \quad (4.10)$$

By substituting values of M_A and M_B from equation [8] in equation [10] and simplifying further the expression for inverse susceptibility becomes,

$$\frac{1}{\chi} = \frac{T}{C} + \frac{1}{\chi_0} - \frac{\sigma}{T-\theta} \quad (4.11)$$

Where

$$C = C_a + C_b$$

$$\frac{1}{\chi_0} = \frac{1}{C^2} (C_a^2 \gamma_{aa} + C_b^2 \gamma_{bb} + 2C_a C_b \gamma_a \gamma_b)$$

$$\begin{aligned} \sigma = \frac{C_a C_b}{C^3} \{ & C_a^2 (\gamma_{aa} - \gamma_{bb})^2 + C_b^2 (\gamma_{bb} - \gamma_{ab})^2 \\ & - 2C_a C_b [\gamma_{ab}^2 - (\gamma_{aa} + \gamma_{bb}) \gamma_{ab} \\ & + \gamma_{aa} \gamma_{bb}] \} \end{aligned}$$

$$\theta = \frac{-C_a C_b}{C} (\gamma_{aa} + \gamma_{bb} - 2N \gamma_{ab})$$

Equation 11 represents the hyperbola which cuts the temperature axis at

$$\theta = \frac{-C}{\chi_0}$$

Where ' θ ' is asymptotic Curie point. The asymptote is given by (as $T \rightarrow \infty$)

$$\frac{1}{\chi} = \frac{T}{C} + \frac{1}{\chi_0} \quad (4.12)$$

∴ The expression for volume susceptibility becomes,

$$\chi = \frac{C}{T+\theta} \quad (4.13)$$

Where, $\theta > 0$

The quantity $\frac{1}{\chi}$ becomes zero at θ where χ becomes theoretically infinity or χ is practically large and the state substance passes from the paramagnetic to ferrimagnetic with decrease in temperature. The substance obeys Curie Weiss law with asymptotic Curie point θ .

ii) Spontaneous Magnetization

At low temperature the magnetizations of the sublattices of ferrimagnetic substance, form the spontaneously magnetized system. The expressions for spontaneous magnetizations are

given by,

$$\text{and } \left. \begin{aligned} M_{\text{Asp}} &= N_a g \mu_b S_a B_a \chi_a \\ M_{\text{Bsp}} &= N_b g \mu_b S_b B_b \chi_b \end{aligned} \right\} \quad (4.14)$$

Where,

B'S are Brillouins functions

N's are the number of atoms per unit volume of appropriate lattices

S's are spin quantum numbers of atoms at appropriate lattices.

$$\chi_a = \frac{S_a \mu_b g}{KT} (\gamma_a M_B - \gamma_{aa} M_A)$$

$$\chi_b = \frac{S_b \mu_b g}{KT} (\gamma_{ab} M_A - \gamma_{bb} M_B)$$

∴ the net spontaneous magnetization can be written as,

$$M = | M_{\text{Bsp}} - M_{\text{Asp}} | \quad (4.15)$$

The graph of M versus T are shown in Figures 4.1 and 4.2. Such curves are of different variety. They provide information about spontaneous magnetization and exchange energy at different temperature. The above theory is supported by experimental curves of Neel [13] Gorter [14] and Smart [15].

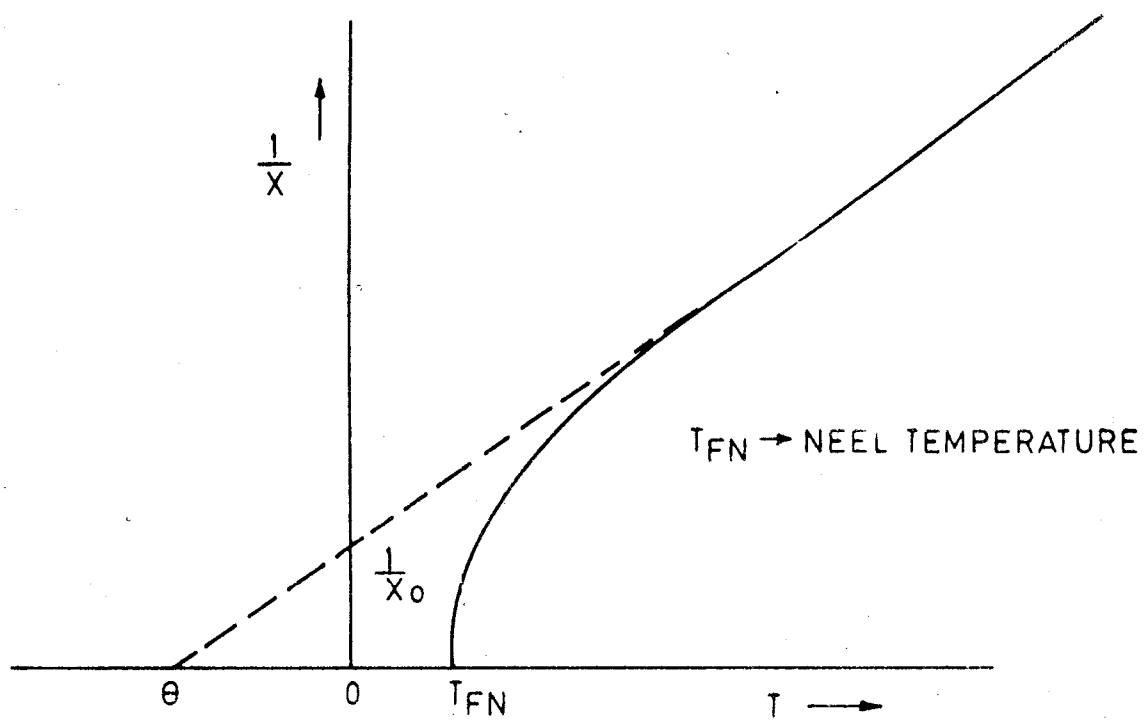


FIG. 4.1 INVERSE SUSCEPTIBILITY ($\frac{1}{X}$) VS TEMPERATURE (T).

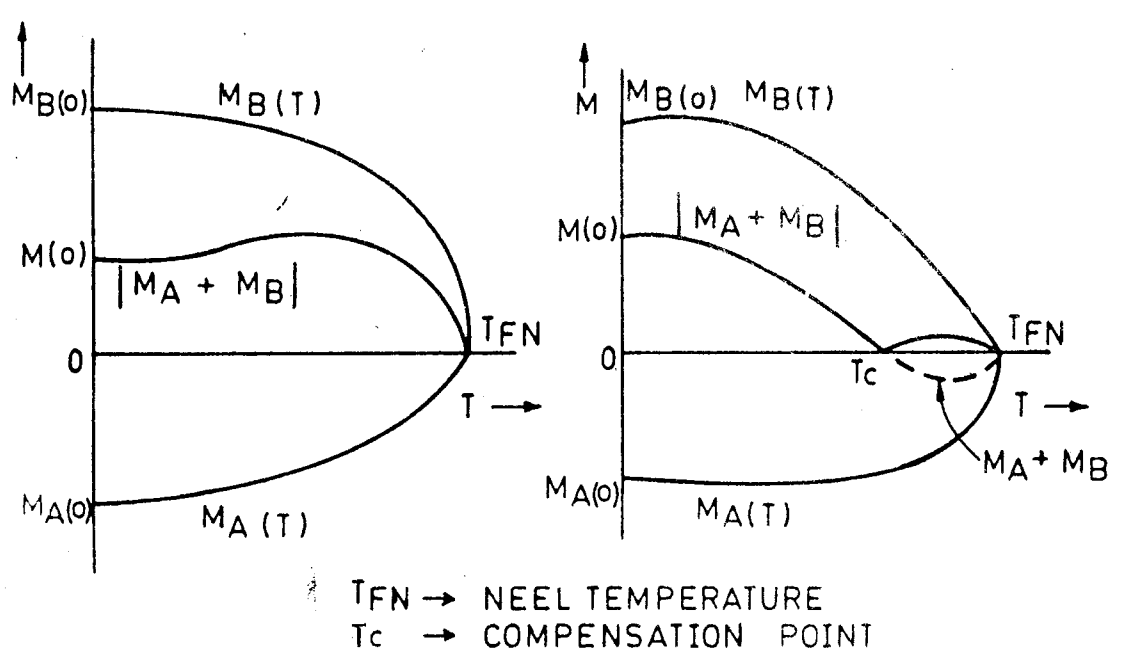


FIG. 4.2 SPONTANEOUS MAGNETIZATION (M) VS TEMPERATURE (T).

4.5 b YAFET - KITTLE THEORY

Neel's theory find its applicability for pure ferrites. But it is inadequate for the spinels which contain other than iron ions. For this Yafet and Kittle [16] proposed triangular type of spin arrangements.

They considered the possibility of subdivision of each lattice to account for the magnetic ordering within the lattice, other than parallel arrangement of spins. When the strong negative interaction exists within the sublattice B, the two equivalent sublattices B_1 and B_2 , being spontaneously magnetized, are not exactly antiparallel. There is a resultant magnetization of B lattice setting antiparallel to the magnetization of A lattice.

The triangular arrangement within the lattice results in values of reduced magnetization of the same order and their magnitude is predicted by Neel's model. They are free from thermodynamic difficulties near absolute zero.

The interaction energy for this case is given by,

$$E = 8 N \left[6J_{ab} S_a S_b \cos \Phi - J_{bb} S_b^2 (2 \cos \Phi - 1) \right] \quad (4.16)$$

Where,

θ = Angle between A and subdivision of B.

j's = Exchange integrals.

Interaction energy is minimum for J_{ab} negative and J_{bb} positive. If $\varphi = 0$ then Neel's state is obtained. If J_{bb} is

also negative, then the ratio of exchange energies is given by,

$$\gamma_{\text{ex}} = \frac{J_{\text{bb}} S_{\text{b}}}{J_{\text{ab}} S_{\text{a}}} > \frac{3}{4} \quad (4.17)$$

Under such condition Neel's state will not be minimum and magnetization of sublattice B_1 and B_2 will be inclined to sublattice A at an angle given by,

$$\cos \phi = \frac{3}{4} \frac{J_{\text{ab}} S_{\text{a}}}{J_{\text{bb}} S_{\text{b}}} \quad (4.18)$$

They proved that Neel's structure is stable for $\gamma_{\text{ex}} < 3/4$, if the total number of sublattices is restricted to six. Further the existence of triangular arrangement has been reported by Lotering [17] in some cases.

4.5. c) SPIRAL SPINS

Lyons and Kaplan [18] have given a generalized treatment of spiral configuration along with Y-K model. They have suggested the possibility of spiral or helical spin arrangements by neutron diffraction in some compounds and showed that, these have lower energy for all values of $\gamma_{\text{ex}} > 2/3$. Corliss and Hastings [19] observed the existence of such configuration in manganese chromite. Similarly spiral spin configuration has been reported by Enz [20] in hexagonal ferrites.

4.6 MAGNETIC HYSTERESIS

Magnetic hysteresis is useful in providing, the information regarding magnetic substances usefulness in industry. Such a loop for virgin ferromagnetic material is shown in fig. 4.3.

When the maximum field strength for loop is small, the magnetization does not increase to its full extent; the loop is lens shaped, its sides are parabolic. When field is increased, at certain critical field it reaches saturation. Upon decreasing the value of saturation field the demagnetization occurs which is not reversible. In other words the susceptibility $\chi = \frac{M}{H}$ is an irreversible function of H.

There exists lag in magnetization with respect to applied field and irreversibility of the path of magnetization, when the field is reversed and decreases to zero. This phenomenon of lagging behind of magnetization with respect to applied field is called as hysteresis.

From the figure 4.1 it can be seen that, increasing the applied field H, induction reaches to saturation value M_s . Upon decreasing the value of applied field to zero, the induction falls to a value M_r , the remanance induction. Reversing the direction of magnetic field and increasing its value causes the induction to fall to zero, defining the coercive force H_c . On further increasing the value of $(-H)$,

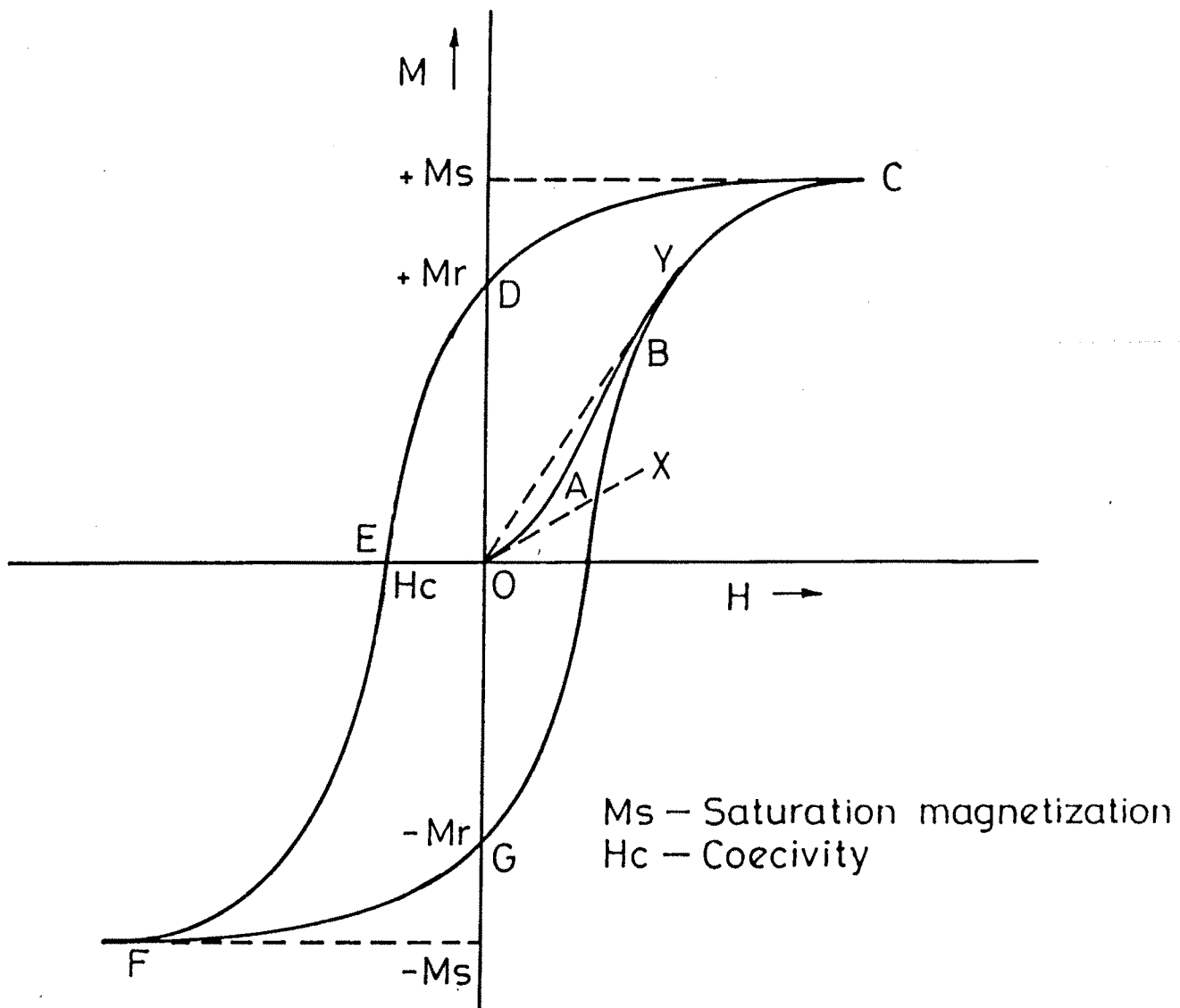


Fig.43-Magnetization curve (OABC) and Hysteresis loop (CDEFGC)

the induction increases in the negative direction to $-M_S$. By decreasing the applied field to zero, the induction does not return on the same path, but rather decreases to a value equivalent to a negative M_r as shown. On reversing and increasing the applied field, the induction falls to zero at a point equivalent to positive H_c . By further increasing H , the loop is closed at M_S . The first path taken by the sample from origin to M_S or OABC is called as the virgin curve or magnetization curve. The part COEFGC is a hysteresis loop. The second quadrant of hysteresis loop is usually called as the demagnetization curve.

4.7 EXPERIMENTAL

The saturation magnetization of ferrites can be measured by ballistic method, vibrating-coil magnetometer, microwave method or a high field loop tracer.

The high field loop tracer which was used in the present case was supplied by M/S Arun Electronics, Bombay. The instrument consists of an electromagnet working on 50 Hz mains supply. The sinusoidal magnetic field, of the order of 3600 Oe in the air gap of about a few mm exists in the instrument. A balancing coil is used to detect the magnetization of the sample kept in the air gap. The experimental set up is as shown in the photograph of fig. 4.4. The signal in the balancing coil is proportional to the magnetic moment of the

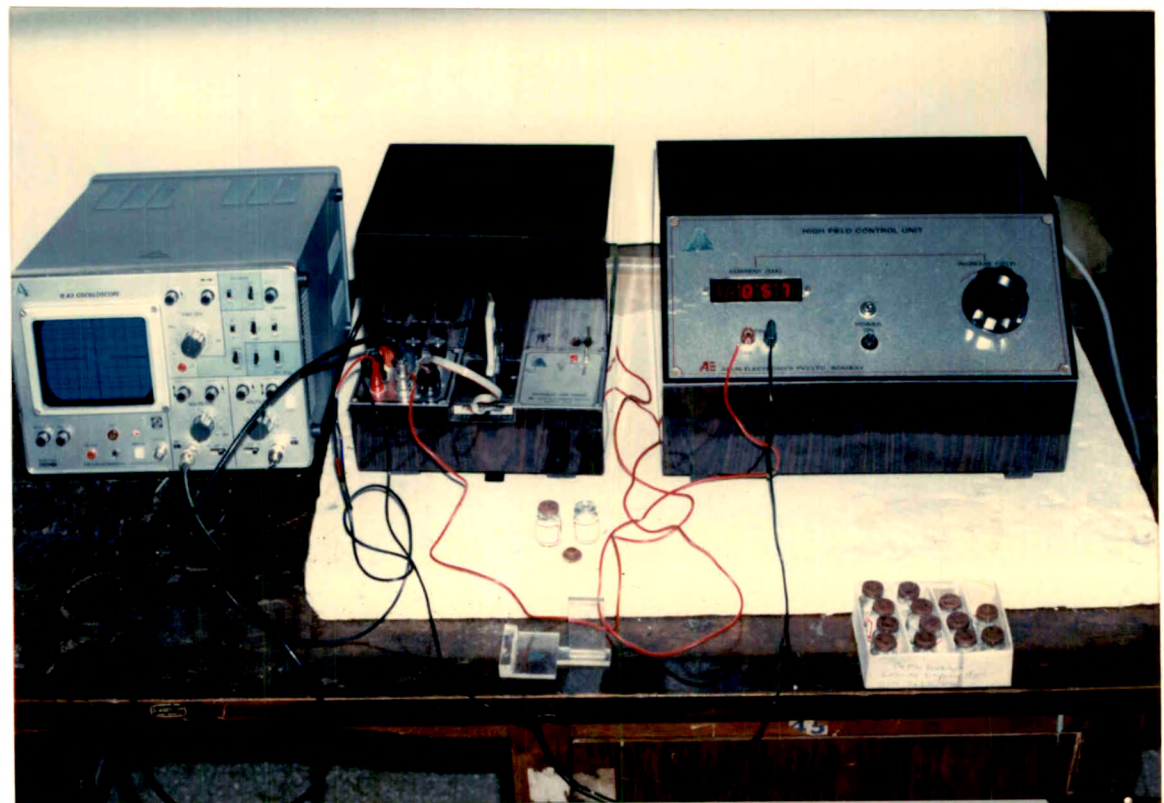


Fig.4.4 EXPERIMENTAL SET UP FOR
HYSTERESIS MEASUREMENT.

BANK. DALAGATED KHANDAKAR LIBRARY
SHIVAJI UNIVERSITY, KOLHAPUR



specimen and this signal is fed to the vertical plates of the oscilloscope with adequate amplification. The signal which is proportional to the applied magnetic field is fed to the horizontal plate of the oscilloscope, and is measured in terms of mv on the digital multimeter.

The apparatus consists of three units:

- i) C-core unit : In this sample under investigation is introduced.
- ii) Control unit : It acts as the power supply and amplifies the signals in C-core unit.
- iii) Display unit : It exhibit the hysteresis loop on CRO. measurements on digital milivoltmeter can be made here.

Initially, the high voltage cable is connected from the control to C-core unit. The balancing coil is slowly introduced into the air gap after connecting it to 12 pin connector associated with C-core unit. The vertical and horizontal outputs of C-core unit are connected to the vertical and horizontal inputs of control unit. The vertical output of control unit is connected to the vertical input of oscilloscope while horizontal to EXT.

With the current control Knob, the minimum current is adjusted so as to obtain the ellipse on the screen. By adjusting horizontal gain potential, the appropriate size ellipse can be obtained.

Saturation magnetization is calculated from the observed reading for the vertical displacement in CRO in terms of milivolts. For the calibration of this displacement, pure nickel in the form of sphere of weight 1.913 gm is loaded between the pole pieces and this gives the reading of 762 mv with the elimination of background noise voltage. The standard magnetization of nickel is $53.54 \times 1.913 = 102.04$ emu. This gives the vertical displacement of 762 mv and therefore the calibration factor is given by $\frac{102}{1010} = 0.10094$ emu per mv.

When the sample in pellet form is fed into the gap between pole pieces, we get some milivolts reading which is denoted by 'C'. The saturation magnetization of the sample is given by,

$$\begin{aligned} \sigma_s &= C \times 0.10094 \quad \text{emu} \\ &= \text{mv} \times \frac{\text{emu}}{\text{mv}} \\ &= \text{-----emu} \end{aligned}$$

or

$$\begin{aligned} \sigma_s' &= \frac{\sigma_s}{\text{weight of the sample}} \\ \sigma_s \left(\frac{\text{emu}}{\text{gm}} \right) &= \frac{\text{emu}}{\text{weight of sample}} \\ &= \text{-----} \end{aligned}$$

The magnetic moment μ_B per molecular formula unit is given by,

$$\mu_B = \frac{\text{molecular weight of sample}}{5585} \times \sigma_s'$$

Magnetization (M_S) is given by the relation,

$$4 \pi M_S = 4\pi(1 - P) dx \sigma_s'$$

where $P = \text{porosity} = \frac{dx - da}{dx}$

where,

$$dx = \text{X ray density} = \frac{8M}{Na^3}$$

where,

$M = \text{Molecular weight of the sample}$

$N = \text{Avagadro's number}$

$$= 6.0225 \times 10^{23} \text{ moles}$$

$a = \text{Lattice parameter of sample}$

$da = \text{Actual density of the sample given}$

by $da = \frac{\text{mass}}{\text{volume}} = \frac{\text{mass of the sample}}{\pi r^2 t}$

where,

$t = \text{Thickness of the sample}$

$r = \text{Radius of the sample.}$

4.8 RESULTS AND DISCUSSION

The data on measurement of porosity is included in table 4.1. The hysteresis loop studies are contained in table 4.2. The calculated values of relevant magnetic properties such as, saturation magnetization and magnetic moment for Mg-Co ferrites sintered at different intervals of time are listed in table 4.3.

T A B L E - 4.1

Porosity data of Mg-Co ferrites

Chemical formula	Sintering temp. and time		Molecular Weight gm	Physical density gm/cc	X ray density gm/cc	Porosity
	Temp., °c	Time, hrs				
MgFe ₂ O ₄	900	20	200.0006	3.18009	4.5147	0.2957
	900	30	200.0006	3.9020	4.5147	0.1350
Mg _{0.6} Co _{0.4} Fe ₂ O ₄	900	20	213.869	3.1816	4.9565	0.3582
	900	30	213.869	3.3797	4.9565	0.3181
CoFe ₂ O ₄	900	20	234.671	4.0211	5.2900	0.2399
	900	30	234.671	4.2242	5.2900	0.2016

T A B L E - 4.2

VERTICAL DISPLACEMENTS IN CRO FOR Mg-Co FERRITES

Sample	Sintering temperature (°c)	Sintering time (hrs)	Vertical displacement mv
MgFe ₂ O ₄	900	20	101
MgFe ₂ O ₄	900	30	127
Mg _{0.6} Co _{0.4} Fe ₂ O ₄	900	20	121
Mg _{0.6} Co _{0.4} Fe ₂ O ₄	900	30	136
CoFe ₂ O ₄	900	20	862
CoFe ₂ O ₄	900	30	905

Table 4.3
MAGNETIZATION DATA OF Mg - Co FERRITES

Sample	Sintering Temp / Oc	Sintering Time hours	Saturation Magnetization			Magnetic Movement M/B Bohr Magnetons
			emu/qm	Ms emv/cc	4π Ms Gauss	
MgFe ₂ O ₄	900	20	29.552	93.960	1180.0	1.058
MgFe ₂ O ₄	900	30	27.040	105.50	1327.0	0.9701
Mg _{0.6} Co _{0.4} Fe ₂ O ₄	900	20	28.690	91.45	2887.0	1.098
Mg _{0.6} Co _{0.4} Fe ₂ O ₄	900	30	28.900	97.83	3088.0	1.106
CoFe ₂ O ₄	900	20	86.94	350.00	4399.0	3.955
CoFe ₂ O ₄	900	30	91.39	386.00	4852.0	4.045

From table 4.3 it is clear that, the saturation magnetization increases with increase in sintering time. The values obtained for saturation magnetization for magnesium ferrites increase, when it is mixed with composition of cobalt. This behaviour can be explained on the basis of redistribution of cations [21], with sintering temperature and time and also on the basis of microstructural changes brought in by firing temperature.

The presence of porosity affects magnetic properties. Due to pores present within the grains, the magnetic contact between the grain decreases hence the increased magnetization with reduced porosity is observed. With increase in sintering time the porosity of each sample is reduced (Table 4.1). This has a considerable effect on the increase of magnetization. This is in confirmation with the reported results [22].

The distribution of grains constituting microstructure gives rise to some resultant magnetic moment. Due to heat treatment [23], grain growth sets in the sample and porosity decreases. Hence at low sintering temperature porosity is relatively high. A pore, an air filled gap within the grains will break up the magnetic contact between grains. The aggregate of large number of pores present in sample at low temperature, results in net reduction of magnetization in bulk of the sample. The grain boundary hinders the movement of

domain walls. The area of grain boundary increases, when number of pores per c.c. are large. This would resist the process of magnetization. When the sample is sintered at high temperature, densification process starts and the net area of grain boundary decreases hence the magnetization increases markedly.

The grain size has an influence on the domain structure of ferrites. When the polycrystalline material consists of grains of larger size, the domain structure corresponds to the single crystal structure. For small grain structure samples, domain structure gets modified due to interaction between the adjacent grains [9]. At lower sintering temperature microstructure/ consists of large number of small sized grains and at higher temperature, densification and grain growth occurs simultaneously, hence microstructure consist of reduced number of grains. Recently Kainuma et al [24] have derived lower limit of grain size in case of soft ferrites, for the appearance of square hysteresis loop by the effect of magnetization and of adjacent grains respectively. Goodenough [25], proposed a domain model for explaining occurrence of a rectangular loop. He assumed that the reverse domain should nucleate at the boundary between two grains with different easy direction to reduce the magnetic energy due to poles appearing at the boundary. Dugar-Zhabon [26], proposed a lower limit of grain size for the occurrence of square loop

by assuming that when mean grain size of a polycrystalline ferrite becomes very small, there exist many grains which cannot have a multidomain structure and therefore squareness ratio (B_r/B_m) should be smaller because distribution in the coercive force becomes wider. Jain [3] et al observed that in manganese zinc ferrites permeability varies directly as the separation of intra-granular pores and the coercive force varies inversely as the square root of this distance. In case of inhomogeneous material having nonmagnetic inclusions, changes in energy in domain wall arises due to change in area of the wall [27]. The variations in magnitude and direction of the magnetization is also contributed to the randomly distributed irregularities within the same domain [28]. When the sintering time is increased, the structure of grain boundaries, inclusions etc may also alter and this may affect the magnetic properties. Depending upon sintering temperature site cation ordering and clusturing of grain boundaries may occur, so as to affect magnetization [29].

Rikukawa [30] has proposed a model which can explain the reduction in magnetization at lower temperature. According to him, demagnetized field is caused by closed pores and closed pore boundaries. At low temperature more pores are present which may form closed pore chain. He gave the expression between permeability, porosity, average grain size and

effective thickness of grain boundary. It appears that at high sintering temperature pores are reduced and effect of formation of closed pore chain is decreased.

The Mg-Co ferrites under investigation have also been studied by Rao and Keer [31], under different sintering conditions. They studied magnetic domain behaviour of $Mg_{1-x}Co_xFe_2O_4$ system ($0 < x < 0.33$). They observed that, the saturation magnetization and coercive field both increases with increase in cobalt content. They have studied the variation of susceptibility with temperature which indicates that magnetic behaviour changes from multidomain to single domain with increase in cobalt content. This is also contributed by the temperature variations of coercive field values. Both these $MgFe_2O_4$ and $CoFe_2O_4$ are cubic spinel and hence Neel's theory can be used to study the magnetic behaviour of these ferrites.

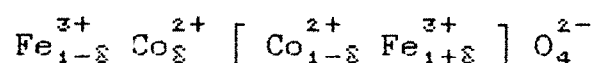
In the present system $MgFe_2O_4$ has negative crystalline anisotropy where as $CoFe_2O_4$ has positive. Rao et al found that interesting variations in coercive field values occur for the mixed system which exemplifies their use in switching phenomenon and memory devices.

Generally, all spinel ferrites are more or less inverse. Some of the divalent metal ions prefer octahedral B site and equal fraction of trivalent iron ions prefer tetrahedral A

sites. The distribution of cations get affected by heat treatment [32]. The degree of inversion, thus vary with firing temperature. The increase in temperature causes the excitation of the ions of the sublattice hence structure changes from normal to inverse. The resultant magnetization is vector sum of sublattice magnetization.

The complete inverse spinel structure of CoFe_2O_4 ferrites has been reported by Prince [33] using neutron diffraction. For completely inverse CoFe_2O_4 the theoretical value of magnetic moment is 3 Bohr magnetons. From table it is observed that the values of Bohr magneton are higher than theoretical value. This is due to the contribution of orbital moment to spin moment and extent of inversion.

Sawatzky et al [34] have reported partial inverse structure of CoFe_2O_4 ; accordingly the cation distribution is given by,



Where ' δ ' is the coefficient of normalancy. The spin moment for Fe^{3+} , Co^{2+} and Mg^{2+} are 5,3,1 Bohr magneton respectively. If the resultant magnetic moment per formula unit is calculated, it comes out to be $3+4\delta$. If this is compaired with observed values of magnetic moment the value of ' δ ' found is 0.24 and 0.26. That is the coefficient of

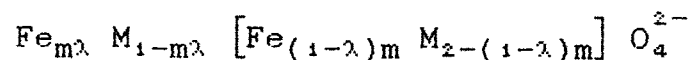
normalancy in cobalt ferrite is 25 to 30% depending on the preparation condition. From the magnetization behaviour of the system under study it can be concluded that for the ferrite samples which are sintered at longer interval of time the saturation magnetization goes on increasing. The increased magnetization is a consequence of microstructural changes that are brought up due to varying sintering time and also due to the changes in the distribution of cations among the sites due to heat treatment.

4.9 Cation distribution in ferrites

Cation distribution is an important aspect of studies in ferrites.

Gilleo [35] has tried to give the general treatment for simple ferrite system involving non magnetic ions.

Gilleo considered the system $M_{3-m}Fe_mO_4$ where M is nonmagnetic ion. Assuming cation distribution



Expression for Curie point becomes

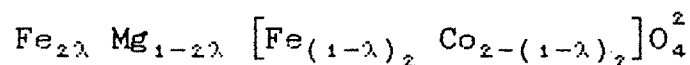
$$T_c(K) = \frac{3\lambda(1-\lambda)F(\lambda_m)g(\lambda_m)mT_o}{2[(1-\lambda).F(\lambda_m) + \lambda g(\lambda_m)]}$$

$$F(\lambda_m) = 1 - [(1-\lambda_m)^5] [(1+5\lambda_m)]$$

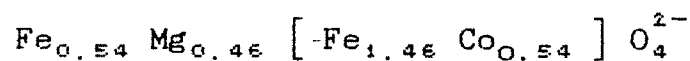
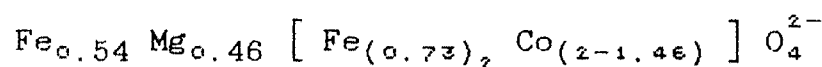
$$g(\lambda m) = 1 - \left[1 - \frac{1}{2} m(1-\lambda) \right]^{11} \left[1 + \frac{11}{2} m(1-\lambda) \right]$$

Where T_0 is a constant.

The constant T_0 was evaluated for standard ferrite. Milligan [36] et al have evaluated T_0 by taking $MgFe_2O_4$ with a distribution $Mg_{.1} Fe_{.9} O_4$ and Curie point $440^\circ C$. T_0 was found to be $962^\circ K$. Gilleo formula is used for calculating the cation distribution. Taking $m = 2$ and the value of observed Curie temperature $T_C = 525^\circ C$, the distribution coefficient λ is found to be 0.27. Since cobalt ferrite is completely inverse, in the sample $Mg_{.6} Co_{.4} Fe_2 O_4$, cobalt prefers B sites where as Mg^{2+} cations prefer A sites. Thus cation distribution according to the above relation may be expressed as



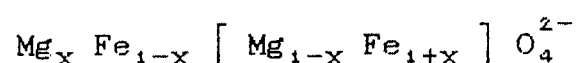
ie



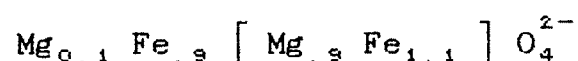
The resultant magnetic moment of the sample using above formula comes out to be 5.74. Since the observed μ_B value is 1.021, Gilleo's formula seems to be not useful in predicting the cation distribution for $Mg_{.6} Co_{.4} Fe_2 O_4$ sample.

The higher value of magnetization can however be explained on the basis of microstructural aspects of this ferrite.

The distribution coefficient ' λ ' for $MgFe_2O_4$ is found to be 0.1, the cation distribution according to relation,



becomes,

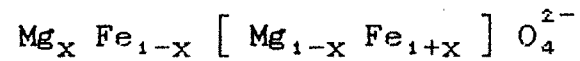


The 'A' site magnetic moment is 4.6 Bohr magnetons and B site magnetic moment is 6.4 Bohr magneton. Hence the net magnetic moment becomes

$$M = | M_B - M_A | = 1.8 \text{ Bohr magneton. The}$$

observed value of magnetic moment is 1.058 Bohr magnetons when sintered for 20 hours and 0.9701 for 30 hours. These are found to be less in comparison with theoretical value. Also it is observed that as sintering time increases in magnesium ferrites magnetic moment decreases, since the relative amount of Mg^{2+} ions on the tetrahedral site will change. The obtained values of Bohr magnetons in $MgFe_2O_4$ may be due to the effect of given heat treatment which changes the site distribution as stated by Neel (1950) and Callen et al [37]. They have studied, the site distribution changes in $MgFe_2O_4$ on appropriate heat treatment and have shown that although

MgFe_2O_4 is an inverse spinel in which most of the Mg^{2+} should occupy the octahedral sites, the molar fraction 'x' of Mg^{2+} ions on the tetrahedral sites in the formula.



depends on the temperature and heat treatment and follows the relationship,

$$\frac{x(1+x)}{(1-x)^2} = \exp(-t/T)$$

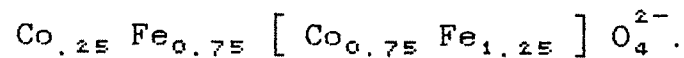
Where 't' is the time and T is absolute temperature.

Epstein and Frackiewicz (1958) [38] have shown that, the variation of t as a function 'x' follows the eqⁿ

$$t = -11.5 \log \frac{x - x^\infty}{x_0 - x^\infty} + 60 (x - x_0)$$

Where x_0 and x^∞ are the starting and equilibrium fraction of Mg^{2+} ions on the tetrahedral sites.

The distribution coefficient λ for CoFe_2O_4 is found to be 0.25. Thus the formula of distribution becomes



Since the 'A' site magnetic moment is $4.50 \mu_B$ and 'B' site magnetic moment is $8.50 \mu_B$. The net magnetic moment for cobalt ferrite thus comes out to be 4.00 Bohr magnetons.

This is equal to the calculated value of magnetic moment. The cobalt ferrite is thus found to be 25% inverse, when it is sintered at 900°C for 30 hrs.

REFERENCES

1. Alpher A.M.
"High Temperature Oxides", Academic Press, N.Y. (1971).
2. Igarashi H., And Chazaki K.
"Effect of porosity and Grain size on magnetic Properties of Ni-Zn Ferrites", J.Am.Ceram.Soc.(USA), Vol.60. No.1-2, P.51-54 (Jan-Feb 1977).
3. Jain G.C., Das B.K., Khonduja R.S. and Gupta S.C.
J.Mat.Sci.(GB) vol.11, No.7, P.1335, 8 (July 1976).
4. Weiss P.L.
"Hypothese Champ Moleculaire, et al propriet Ferromagnetique", J.de Phisique, 6, P 661 (1907).
5. Kittle Charles
"INtroduction to Solid State Physics" 5th Ed. Wiley Eastern Ltd. P.460 (1979).
6. Cullity B.D.
"Introduction to Magnetic Materials" Addison Wesley Publ.Co, P.131 (1972).
7. Heisenberg W.
"On the theory of ferromagnetism" Zent fur Phys, 49 P.619 (1928).
8. Landau L. and Lifshitz
Physik Z.Sowje tunion Vol.8 P:153 (1935).
9. Craik D.J., and Griffith's P.M.
Brit.J.Appl.Phys. Vol.9, P.905 (1958).
10. Hundson A.S. and Iceram M.A.
"Review of microwave ferrites and Garnets" The Marconi Review P-155 (1st Sept 1970).
11. Brailsford F.
"Physical Principles of Magnetism" D. Van Nostrand Co. P.202 Feb(1960).
12. Morrish A.H.
"The Physical principles of Magnetism" John Wiley and Sons Inc. (1967).
13. Neel L.
Ann. Phy.(paries) 301-3 P.137 (1978).

14. Gorter E.W. and Schulkes
J.Appl.Phy.Rev. Vol.90, P.487(1953).
15. Smart J.S.
Amer.J.Phy. Vol.23, P.356 (1955).
16. Yafet W. and Kittle C.
Phy.Rev. Vol.87, P.290 (1952).
17. Lotgering F.K.
Phillips. Res.Rept. Vol.11, P.190 (1956).
18. Lyons, D.H. and Kaplan T.A.
Phy.Rev. Vol.120, P.1580 (1960).
19. Corliss L. and Hastings J.
J.Appl.Phy. Vol.335, P.1138 (1962).
20. Enz V.
Appl.Phy. Vol.325, P.22 (1961).
21. Pukhar I.K., Davido Vich A.G., and Zivovik M.A.
Iud. Lab(USA) Vol.40, No.4, (P.511-13 April 1974).
22. Muncheol Poek Ho
Bin. Im.SU.II Pyan. Trans Korean Institute. Electr.Eng.
Vol.32, No.1, P.24-29 (1983).
23. Burke J.E.
"Kinetics of high temperature processes"
Ed. Kingery E.D. N.Y. P.109 (1959).
24. Kainuma S.
J.Appl.Phy. Vol.18, No.12 (Dec. 1979).
25. Goodenough J.B.
Phy.Rev. Vol.95, P.917 (1954).
26. Dugar K.D. Zhabon
Sov.Phy.Solid State, Vol.13, P.1837 (1972).
27. Kerstem M.
Hirzel Lefpzing (1963).
28. Neel L.
"Magnetic properties of ferromagnetism and
antiferromagnetism". Ann.Physique 3, p.37 (1948).
29. Vogel R.H. and Evans B.J.
AIP conf. Proc.(USA) No.34, P.125-7 (1976).

30. Rikukuwa H.
IEEE Trans Magn. (USA) Vol.18, No.6, P-1535-7, (Nov 1982)
31. Rao Venkatesh, and Keer H.V.
"Magnetic Domain behaviour of $MgFe_2O_4-CoFe_2O_4$ System"
Pramana, Vol.19, No.1, P.103-106 (July 1982).
32. Rezlescu N.
Phys.Status Solidi A (Germany), Vol.2, No.2,
P.81-4. (June 1970).
33. Prince E.
"Neutron diffraction results of heat treatment in
Cobalt Ferrites", Phy.Rev. Vol.102, P.674-76 (1956).
34. Sawatzky G.A., Vander Woude F., and Morrish A.H.
J.Appl.Phy. Vol.39. P.1204-6 (1968).
35. Gilleo M.A.
J.Phy.Chem.Solids (GB), Vol.113, P.33 (1960).
36. Milligan W.O., Tamai Y. and Richardson J.T.
J.Appl.Phy. Vol.34 P.2093 (1963).
37. Schieber M.M.
"Experimental Magnetochemistry of non metallic magnetic
materials", Ed. Wolhfarth Vol VIII P.89 (1967).

...Oo*oO...